Exploratory Research and Hypothesis in Medicine **2025** vol. 10(1) | 14–24
DOI: 10.14218/ERHM.2024.00036

Original Article

Role of ELK3 in Ferroptosis of Rheumatoid Arthritis Fibroblast-like Synoviocytes

Yaqun Zhang, Huimin Shi, Lin Wang and Jihong Pan*

School of Biomedical Sciences, Shandong First Medical University & Shandong Academy of Medical Sciences, Shandong Medical Biotechnology Center, Jinan, Shandong, China

Received: October 24, 2024 | **Revised:** November 20, 2024 | **Accepted:** December 06, 2024 | **Published online:** January 20, 2025

Abstract

Background and objectives: Rheumatoid arthritis (RA) is an inflammatory arthritis characterized by chronic joint inflammation, cartilage degradation, and bone erosion. ELK3 is a transcriptional repressor that can affect cell proliferation, migration, invasion, apoptosis, and other cellular processes. The study aimed to clarify the effect of ELK3 in the biological activity and ferroptosis phenotype of RA fibroblast-like synoviocytes (FLS), and to reveal its molecular mechanism in regulating ferroptosis in RA FLS.

Methods: We investigated the impact of ELK3 on the biological activity and ferroptosis phenotype of RA FLS using real-time quantitative polymerase chain reaction, immunohistochemistry, Transwell assay, CCK-8 assay, and ferroptosis-related indicator kit. The molecular mechanism of ELK3 in RA FLS was further explored using Western blot, chromatin immunoprecipitation polymerase chain reaction, and other experiments.

Results: ELK3 was highly expressed in RA. Silencing ELK3 inhibited the invasion and proliferation of RA FLS (both $p < 0.05$). After silencing ELK3 in imidazole ketone erastin-induced RA FLS, intracellular reactive oxygen species, lipid peroxidation levels, ferrous ion content, 4-Hydroxynonenal levels, and Malondialdehyde concentrations all increased. Additionally, ELK3 affects ferroptosis in RA FLS by regulating kelch-like ECH-associated protein 1 ($p < 0.05$).

Conclusions: Silencing ELK3 leads to decreased invasion and proliferation of RA FLS, affecting their biological activity. ELK3 inhibits ferroptosis by suppressing its transcriptional activity through binding to the kelch-like ECH-associated protein 1 promoter. This suggests that ELK3 may be a potential target for RA therapy.

Introduction

Rheumatoid arthritis (RA) is a common inflammatory arthritis, characterized by inflammatory changes in the joints, cartilage, and synovial tissues.[1,2] The prevalence of RA is 0.5–1%, and it can occur at any age, with a high rate of disability.[3,4] In RA, fibroblast-like synoviocytes (FLS) are commonly found at the pannus-cartilage junction. These cells exhibit tumor-like behavior and are considered key factors in the onset and progression of RA.[5–8] RA FLS proliferate excessively, producing an overabundance of matrix metalloproteinases, leading to bone destruction and giving the cells an invasive phenotype.[9] Recent studies suggest that ferroptosis occurs in RA. Ferroptosis is a form of cell death caused by excessive accumulation of lipid peroxides due to metabolic pathway dysfunction.[10] Among the many factors, dysregulation of iron and lipid metabolism has been implicated in regulating the pathological characteristics of RA.[11] Previous studies have found higher iron content in RA synovial fluid compared to osteoarthritis patients and healthy individuals, while serum iron levels are lower in RA patients.[12] Ferroptosis, a novel form of iron-dependent lipid peroxidation-mediated cell death, has garnered attention in recent years as a potential approach to treating cancer cell drug resistance.[13] However, its role in RA disease progression remains unclear.

Nuclear factor erythroid 2-related factor 2 (Nrf2) plays a central role in suppressing ferroptosis. Many ferroptosis-related genes are transcriptionally regulated by Nrf2.[14] Our research also found that *in vitro* treatment with the ferroptosis inducer IKE induced

Keywords: Rheumatoid arthritis; Fibroblast-like synoviocytes; ELK3; Ferroptosis; Kelch-like ECH-associated protein 1; Nuclear factor erythroid 2-related factor 2.

***Correspondence to:** Jihong Pan, Biomedical Sciences College & Shandong Medicinal Biotechnology Center, Shandong First Medical University & Shandong Academy of Medical Sciences, No. 6699, Qingdao Road, Jinan, Shandong 250117, China. ORCID: https://orcid.org/0000-0002-3130-0044. Tel: +86-0531-59567366, E-mail: panjihong@sdfmu.edu.cn

How to cite this article: Zhang Y, Shi H, Wang L, Pan J. Role of ELK3 in Ferroptosis of Rheumatoid Arthritis Fibroblast-like Synoviocytes. *Explor Res Hypothesis Med* 2025;10(1):14–24. doi: 10.14218/ERHM.2024.00036.

© 2025 The Author(s). This article has been published under the terms of Creative Commons Attribution-Noncommercial 4.0 International License (CC BY-NC 4.0), which permits noncommercial unrestricted use, distribution, and reproduction in any medium, provided that the following statement is provided. "This article has been published in *Exploratory Research and Hypothesis in Medicine* at https://doi.org/10.14218/ERHM.2024.00036 and can also be viewed on the Journal's website at https://www.xiahepublishing.com/journal/erhm".

Table 1. Primer sequences

Gene name	Forward(5′→3′)	Reverse(5′→3′)
GAPDH	GGAGCGAGATCCCTCCAAAAT	GGCTGTTGTCATACTTCTCATGG
ELK3	GACGTCACCCGTTCT GTT G	AGGCAAATTTTGGTGTACGG
KEAP1	CTGGAGGATCATACCAAGCAG	GGATACCCTCAATGGACACCAC
PTGS2	ATGCTGACTATGGCTACAAAGC	TCGGGCAATCATCAGGCAC
SLC7A11	GGTCCATTAGCTTTTGTACG	AATGTAGCGTCCAAATGCCAG
GPX4	GAGGCAAGACCGAAGTAAACTAC	CCGAACTGGTTACACGGGAA
NQO1	TCAGCCAATCAGCGTTCGGTATTAC	AAATAGACGGGGACTCCCGA
Nrf2	CCGCCTCTAAGTTCTTGTCCC	GCGGAGAACTAGGAGATAGCC
ACSL4	ATCGTAATTGGTGGACAGAACA	ACTCTCCTGCTTGTAACTTCAC

ferroptosis in RA FLS, increasing Nrf2 expression. Our predictive analysis revealed a close correlation between ELK3 and Nrf2 expression, leading us to hypothesize that ELK3 may be involved in RA FLS ferroptosis by regulating Nrf2 or its related molecules.

ELK3 is a member of the ternary complex factors.[15] Current research has shown that ELK3 is upregulated in various cancers, suggesting its potential oncogenic role. ELK3 influences behaviors such as invasion, migration, proliferation, and cell cycle progression in cancer cells, including those from breast cancer,[16] glioma,[17] and pancreatic cancer.[18] However, research on ELK3 outside the field of oncology is limited, and its relationship with RA has not been reported. In our RNA-seq analysis of RA FLS treated with IKE, we found increased expression of ELK3 under IKE stimulation. Using the GeneCards database, we discovered a close relationship between ELK3 and Nrf2. Since Nrf2 is closely related to ferroptosis, we speculate that ELK3 may be involved in the occurrence of ferroptosis in RA. While ferroptosis has been observed in RA, its specific impact on disease progression remains unclear. Therefore, this study aimed to clarify the expression of ELK3 in RA, its effect on the biological activity and ferroptosis phenotype of RA FLS, and the specific mechanisms involved.

Materials and methods

Cell source and culture

The RA synovial tissues and osteoarthritis (OA) synovial tissues used in this study were collected from knee joint synovial tissues removed during clinical replacement surgeries at Shandong First Medical University's affiliated hospital. Samples were obtained from 12 RA patients and six OA patients (aged 35–70). The study received informed consent from each patient and approval from the Medical Ethics Committee of the Shandong Medical Biotechnology Center (Ethics Approval No.: 2014-2019). All patients met the revised RA diagnostic criteria established by the American College of Rheumatology in 1987. The research process complies with the principles of the Helsinki Declaration.The synovial tissue was minced using sterile scissors and digested in 300 μL type II collagenase (Solarbio, C8150) and 2 mL type III collagenase (Solarbio, C8490) at 37°C in 5% CO2 for 6–8 h. After digestion, the supernatant was discarded, and the remaining material was cultured for 24–48 h. Adherent cells were retained, and non-adherent cells and debris were removed. The cells were washed with phosphate-buffered saline (PBS), and fresh complete medium was added for further culture in an incubator. The culture medium used was DMEM (Gibco) containing 15% fetal bovine serum (FBS) and 1% penicillin-streptomycin. The cells were passaged and used between passages 3–8.

Real-time quantitative polymerase chain reaction (RT-qPCR)

Total RNA was extracted from treated cells using Trizol (Vazyme, R401-01) according to the reagent instructions, and reverse transcribed into cDNA using a reverse transcription kit (Vazyme, R223-01). RT-qPCR was performed using a fluorescent quantitative PCR instrument (Roche LightCycler 480) with the following conditions: 95°C pre-denaturation for 10 m, 95°C denaturation for 15 s, 60°C annealing/extension for 1 m, repeated for a total of 40 cycles. The experiment was repeated three times, and the mRNA expression level of the target gene was calculated using the $2^{-\Delta\Delta Ct}$ method. Primer sequences are shown in Table 1.

Measurement of RA FLS invasion and proliferation

RA FLS (6×10^5 cells) were seeded in 12-well plates and divided into a negative siRNA (siNC) control group and an siELK3 group (RiboBio, stB0006239C). After 24 h of ELK3 interference, the following experiments were conducted. Each group had three replicates.

RA FLS Invasion Measurement: Matrigel was diluted with DMEM (Matrigel:DMEM = 1:7) and evenly applied to the upper chamber. The chamber was placed in a 37°C incubator with 5% CO2 for about 1 h. Cells were seeded at a density of 5×10^4 cells/mL in the upper chamber with DMEM containing 2% FBS. After cell adhesion, 500 μL of DMEM with 15% FBS was added to the lower chamber, and overnight culture was performed to form a concentration gradient. After staining the cells in the lower chamber, invasion cells were counted under a microscope.

RA FLS Proliferation Measurement: Cell proliferation was measured using a CCK-8 assay (Solarbio). Cells were treated similarly to the invasion assay, seeded at a density of 2×10^3 cells/well in 96-well plates. At 0 h, 24 h, 48 h, and 76 h, 110 μL of DMEM containing 10% CCK-8 was added to each well. After incubating at 37°C in the dark for 50 m, absorbance was measured at 450 nm using a microplate reader (SpectraMax iD3). Data were processed using GraphPad Prism 9.

Western blot

RA FLS were seeded in six-well plates and treated according to the experimental purpose. Cells were collected after 48 h. The cells were lysed using RIPA lysis buffer containing PMSF protease inhibitors (RIPA:PMSF = 100:1), and the protein concentration was determined. SDS-PAGE electrophoresis was performed under the

following voltage conditions: 66 V for 10 m, 76 V for 20 m, and 126 V for 1 h. Once the proteins reached the bottom, they were transferred to a 0.45 μm PVDF membrane under 250 mA for 1 h. After blocking with 5% skim milk in TBST for 1 h, primary antibodies were incubated overnight at 4°C. The membranes were washed with TBST three times, followed by incubation with secondary antibodies for 1 h at room temperature. After washing the membranes again, ECL Plus detection was used for visualization. ImageJ software was used for analysis.

siELK3 and ELK3 adenovirus (Adv-ELK3) transfection

siRNA Transfection: siRNA was prepared by mixing HePerfect (Qiagen, 301705) (3 μL), siRNA (3 μL), and 100 μL of serum-free medium (for a 24-well plate). The mixture was incubated at room temperature for 10 m. 400 μL of complete medium was added to each well, followed by the siRNA mixture. The siRNA sequences were: siELK3 (homo): 5′-GCCAAACGCTGCCAGTATT-3′; siKeap1 (homo): 5′-CTACGATGTGGAAACAGA-3′.

Adv-ELK3 Overexpression Transfection: For a 24-well plate, the appropriate volume of the virus was calculated based on the number of cells to be infected (added virus volume (mL) = MOI × number of cells/virus titer (TU/mL), with MOI set to 1,000). 2 μL of Adv-HR transfection reagent was added to each well to enhance infection efficiency. After 6 h of incubation, the viral medium was removed, and a fresh complete medium was added for continued culture.

Detection of lipid peroxidation using C11 BODIPY 581/591 probe, iron ion content detection, and reactive oxygen species (ROS) detection

RA FLS were seeded in 6-well plates and divided into the following groups: siNC, siELK3, siNC + IKE (ferroptosis inducer), and siELK3 + IKE. After 24 h of treatment, the following experiments were conducted.

Lipid Peroxidation Detection: Lipid peroxidation was assessed using the C11 BODIPY 581/591 probe (Thermo Fisher Scientific, D3861) according to the manufacturer's instructions. Fluorescence was observed using a confocal microscope, with excitation at 488–565 nm to observe oxidized and reduced fluorescence states.

Iron Ion Content Detection: Cells were treated and grouped as described above. The BioTracker 575 Red Fe^{2+} Dye Kit (Sigma-Aldrich, SCT030) was used according to the manufacturer's instructions. Fluorescence was observed using a confocal microscope.

ROS Detection: ROS detection was performed using a ROS detection kit (Beyotime, S0033S). Cells were treated as described above, with a positive control (Rosup) added to the wells. The DCFH-DA probe was diluted 1,000-fold and added to the cells for 20 m at 37°C in the dark. 4′,6-diamidino-2-phenylindole was used for nuclear staining, and ROS were observed using a confocal microscope.

Measurement of malondialdehyde (MDA) content and 4-Hydroxynonenal (4-HNE) enzyme-linked immunosorbent assay

RA FLS were seeded in 12-well plates, with no fewer than 3×10^6 cells per well. Cells were divided into siNC and siELK3 groups.

MDA Content Detection: MDA content was measured using an MDA detection kit (Elabscience, E-BC-K028-M) following the manufacturer's instructions. The optical density (OD) value at 532 nm was detected using a microplate reader. The formula for calculating MDA content is: MDA (nmol/mgprot) = ΔA1/ΔA2×C×f÷Cpr, where: ΔA1 = OD value of the sample tube – OD value of the blank tube; ΔA2 = OD value of the standard tube – OD value of the blank tube; C = standard concentration (10 nmol/mL); f = dilution factor of the sample; Cpr = protein concentration of the sample (mgprot/mL).

4-HNE Enzyme-Linked Immunosorbent Assay: Cells were treated and grouped as described above. After 24 h of treatment, the supernatant was collected, and the 4-HNE enzyme-linked immunosorbent assay was performed following the manufacturer's instructions (Jianglai Bio, JL46304). The OD value at 450 nm was detected using a microplate reader.

Chromatin immunoprecipitation PCR and dual luciferase reporter gene assay

Cells were cultured in T75 flasks and divided into siNC and siELK3 groups. ChIP experiments were performed according to the manufacturer's instructions (Beyotime, P2078). DNA was purified using a DNA purification kit (Tiangen, DP204). The purified DNA was amplified using PCR. PCR reaction conditions: 94°C for 5 m (pre-denaturation), 94°C for 30 s, 55°C for 30 s, and 72°C for 30 s per kb for 35 cycles, followed by 72°C for 7 m. The amplification products were subjected to agarose gel electrophoresis, with a voltage of 100–120 V and a current of 300 mA, stopping when the band was 1 cm from the bottom of the gel. The gels were imaged using a gel imaging system.

For the dual luciferase reporter gene assay: 293T cells were seeded in 24-well plates. Once the cells reached 60–70% confluency, plasmids containing the kelch-like ECH-associated protein 1 (Keap1) promoter were transfected. After 24 h, ELK3 plasmids and empty plasmids were added to the experimental and control groups, respectively. After 24–36 h of incubation, the cells were collected and lysed. Luciferase activity was measured using a dual luciferase reporter assay kit (Promega, E1910). OD values at 560 nm for firefly luciferase and 465 nm for Renilla luciferase were detected using a microplate reader. Transcriptional activity was calculated by the ratio of OD values at 560 nm to 465 nm.

Cell fluorescence

RA FLS were seeded in 48-well plates and divided into siNC and siELK3 groups. Fixed cells were treated with 4% paraformaldehyde for 15 m, washed with PBS three times, and then permeabilized with Triton X-100 (Triton X-100: PBS = 1:1,000) for 10–15 m. Cells were blocked with 5% BSA at 37°C for 1 h and incubated overnight with primary antibodies at low temperature. The following day, the cells were incubated with secondary antibodies and stained with DAPI. Fluorescence was observed using a confocal microscope.

Statistical methods

Data were processed using GraphPad Prism 9. T-tests were used for single-factor variables, and ANOVA was applied for the analysis of two or more samples. Statistical significance was determined with $p < 0.05$.

Results

Effect of ELK3 on RA FLS biological activity

As shown in Figure 1, ELK3 mRNA levels in RA FLS were significantly higher than those in OA (Fig. 1a, $n = 3$, $p < 0.01$), and ELK3 expression in RA synovial tissues was also higher than in OA (Fig. 1b, $n = 3$, $p < 0.01$). After screening small interfering ELK3, silencing ELK3 significantly reduced ELK3 mRNA expression ($p < 0.0001$) (Fig. 1c). Co-transfection with siELK3-1

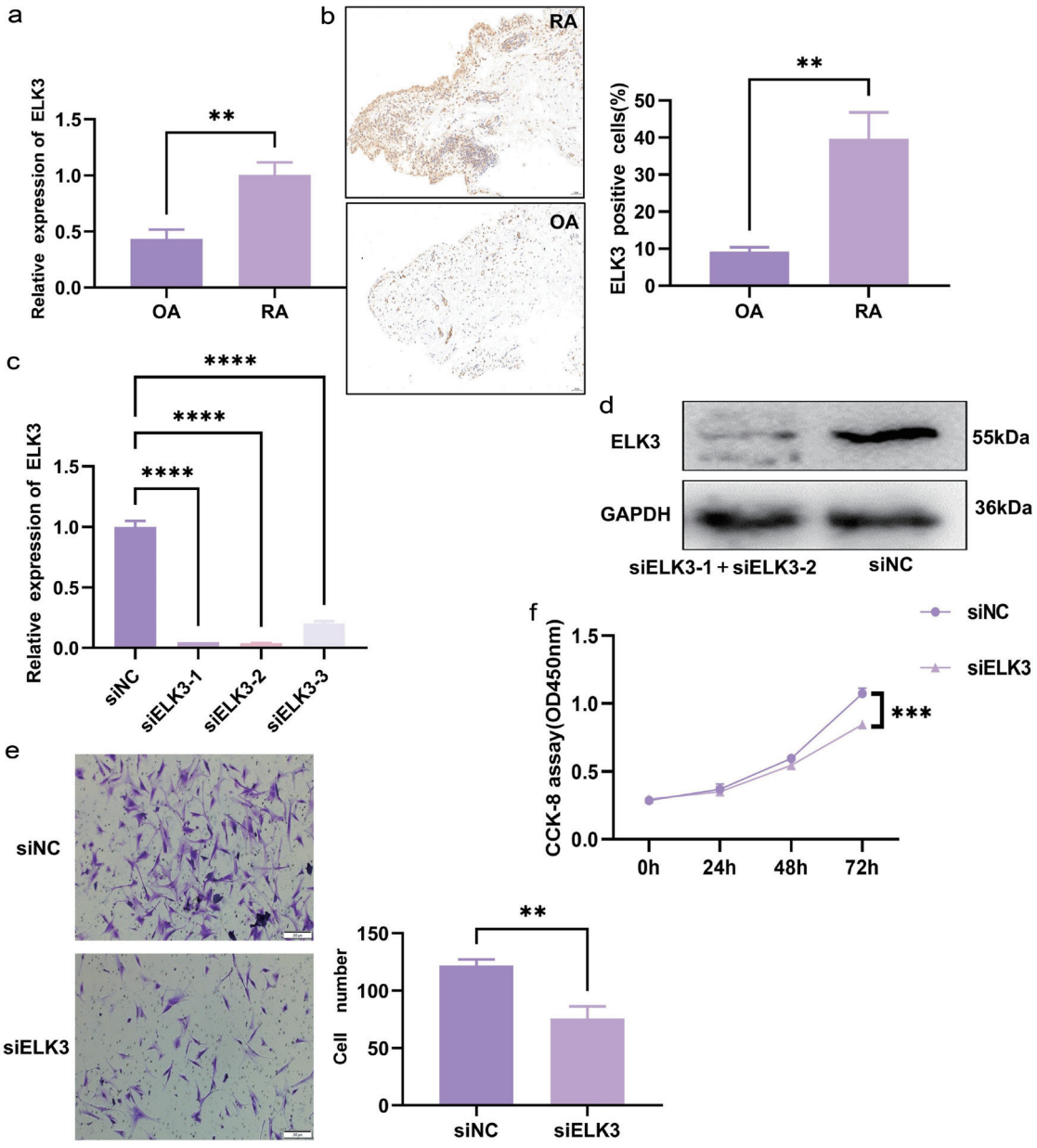

Fig. 1. Effect of ELK3 on the biological activity of rheumatoid arthritis (RA) fibroblast-like synoviocytes (FLS). (a) Expression levels of ELK3 mRNA are significantly higher in RA FLS compared to osteoarthritis (OA) FLS. (b) The expression of ELK3 in the synovial tissue of RA is higher than that in OA. Scale bar: 50 μm. (c, d) After transfection of siELK3 into RA FLS, the expression of ELK3 was significantly reduced, with siNC used as a negative control. (e) Effect of ELK3 silencing on cell invasion ability: Scale bar: 200 μm. (f) Effect of siELK3 on the proliferation of RA FLS was detected. Results are expressed as mean ± SEM from three independent experiments: *$p < 0.05$, **$p < 0.01$, ***$p < 0.001$, ****$p < 0.0001$. SEM, standard error of the mean.

and siELK3-2 also significantly reduced ELK3 protein levels (Fig. 1d). Subsequent experiments used co-transfection of siELK3-1 and siELK3-2. Transwell and CCK-8 assays showed that silencing ELK3 inhibited the invasion and proliferation of RA FLS ($p < 0.01$) (Fig. 1e, f).

Effect of ELK3 on the expression of ferroptosis-related molecules in RA FLS

RA FLS were stimulated with the ferroptosis inducer IKE (10 mmol/L) for 24 h, and the expression level of ELK3 in RA FLS was significantly increased ($p < 0.001$) (Fig. 2a). To verify the relationship between ELK3 and ferroptosis in RA FLS, RT-qPCR was used to detect the effect of ELK3 silencing on the expression of ferroptosis-related molecules in RA FLS. After silencing ELK3, the mRNA level of prostaglandin-endoperoxide synthase 2 (PTGS2) increased ($p < 0.01$), while the expression of solute carrier family 7 member 11 (SLC7A11) decreased ($p < 0.001$), and these trends remained unchanged when IKE was added (Fig. 2b). In contrast, overexpression of ELK3 resulted in an increase in glutathione peroxidase 4 (GPX4) expression ($p < 0.0001$) and

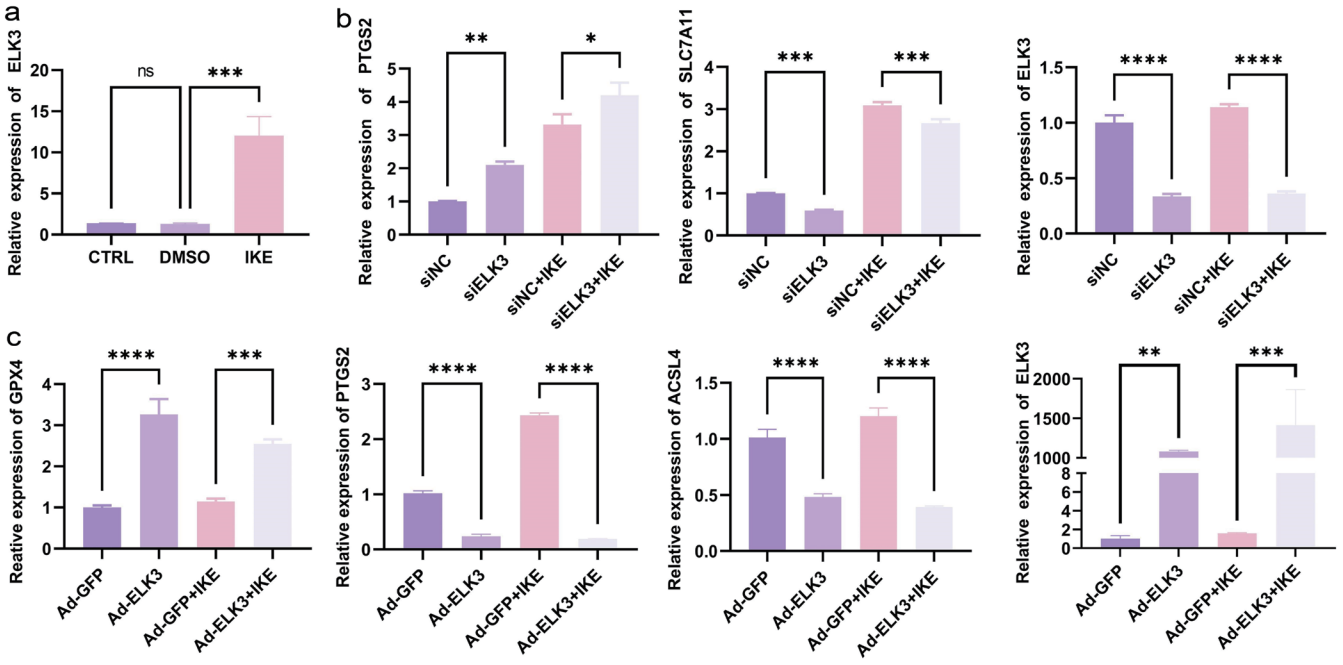

Fig. 2. Effect of ELK3 on the expression of ferroptosis-related molecules in rheumatoid arthritis (RA) fibroblast-like synoviocytes (FLS). (a) RA FLS were treated with imidazole ketone erastin (IKE) (10 mmol/L, 24 h), and ELK3 mRNA expression levels were elevated. (b, c) ELK3 was silenced or overexpressed in RA FLS, with or without IKE induction and real-time quantitative polymerase chain reaction (RT-qPCR) was used to detect the expression of PTGS2, SLC7A11, GPX4, and ACSL4. Results are expressed as mean ± SEM from three independent experiments: *$p < 0.05$, **$p < 0.01$, ***$p < 0.001$, ****$p < 0.0001$. CTRL, control; SEM, standard error of the mean.

a decrease in PTGS2 and acyl-CoA synthetase long-chain family member 4 expression ($p < 0.0001$), with these trends also remaining unchanged upon IKE induction (Fig. 2c).

Effect of ELK3 on lipid peroxidation in RA FLS

The results showed that both with and without IKE induction, silencing ELK3 increased the fluorescence ratio of oxidized (O-BODIPY) to reduced (R-BODIPY) states in RA FLS ($p < 0.05$) (Fig. 3a). Additionally, silencing ELK3 significantly increased the levels of lipid peroxidation products 4-HNE ($p < 0.001$) and MDA ($p < 0.05$) in RA FLS (Fig. 3b, c).

Effect of ELK3 on Fe^{2+} and ROS levels in RA FLS

The results showed that, compared to the control group, silencing ELK3 significantly increased the Fe^{2+} content in RA FLS ($p < 0.001$). When IKE was added, the Fe^{2+} content increased even further ($p < 0.0001$) (Fig. 4a). Additionally, ROS levels in RA FLS were detected, and the results showed that silencing ELK3 led to a significant increase in ROS levels in RA FLS, both with and without IKE induction ($p < 0.05$) (Fig. 4b).

Study on the mechanism of ELK3 in regulating ferroptosis in RA FLS

As a transcriptional repressor, ELK3 is involved in regulating the transcription of various genes. To identify downstream genes regulated by ELK3, we used the UCSC Genome Browser to search for potential promoter sequences and scored the interaction between ELK3 and potential promoters using the JASPAR website. The results showed that Keap1 had the highest score, leading us to hypothesize that ELK3 may regulate ferroptosis by controlling the expression of Keap1.

ELK3's regulation of ferroptosis-related markers

RA FLS were transfected with either siELK3 or Adv-ELK3 to silence or overexpress ELK3, respectively. Western blot, RT-qPCR, and immunofluorescence assays showed that overexpression of ELK3 downregulated Keap1 ($p < 0.0001$) and upregulated Nrf2 ($p < 0.01$) and GPX4 ($p < 0.01$). Conversely, silencing ELK3 increased Keap1 expression ($p < 0.001$) and reduced the expression of Nrf2 ($p < 0.05$) and GPX4 ($p < 0.05$) (Fig. 5a–d). Immunofluorescence analysis also confirmed that silencing ELK3 increased Keap1 expression ($p < 0.05$) (Fig. 5e).

ELK3 regulates ferroptosis in RA FLS by controlling Keap1

To explore the mechanism by which ELK3 regulates Keap1 expression, Chromatin immunoprecipitation PCR experiments were conducted, demonstrating that ELK3 binds to the Keap1 promoter region ($p < 0.0001$) (Fig. 6a, b). Dual-luciferase reporter gene experiments further revealed that ELK3 inhibits Keap1 promoter activity (Fig. 6c). Additionally, western blot analysis showed that Keap1 downstream molecules, including NAD(P)H quinone dehydrogenase 1 (NQO1), were reduced when ELK3 was silenced and increased when ELK3 was overexpressed ($p < 0.05$) (Fig. 6d). Rescue experiments confirmed that co-silencing Keap1 and ELK3 partially restored the expression of NQO1, SLC7A11, and Nrf2 (Fig. 6e).

Discussion

RA is a chronic inflammatory autoimmune disorder that leads to varying degrees of damage to joints and extra-articular organs.[1,19] Due to the complexity of the disease, current clinical treatments for RA primarily involve joint replacement surgery and the administration of disease-modifying antirheumatic drugs.[20,21] How-

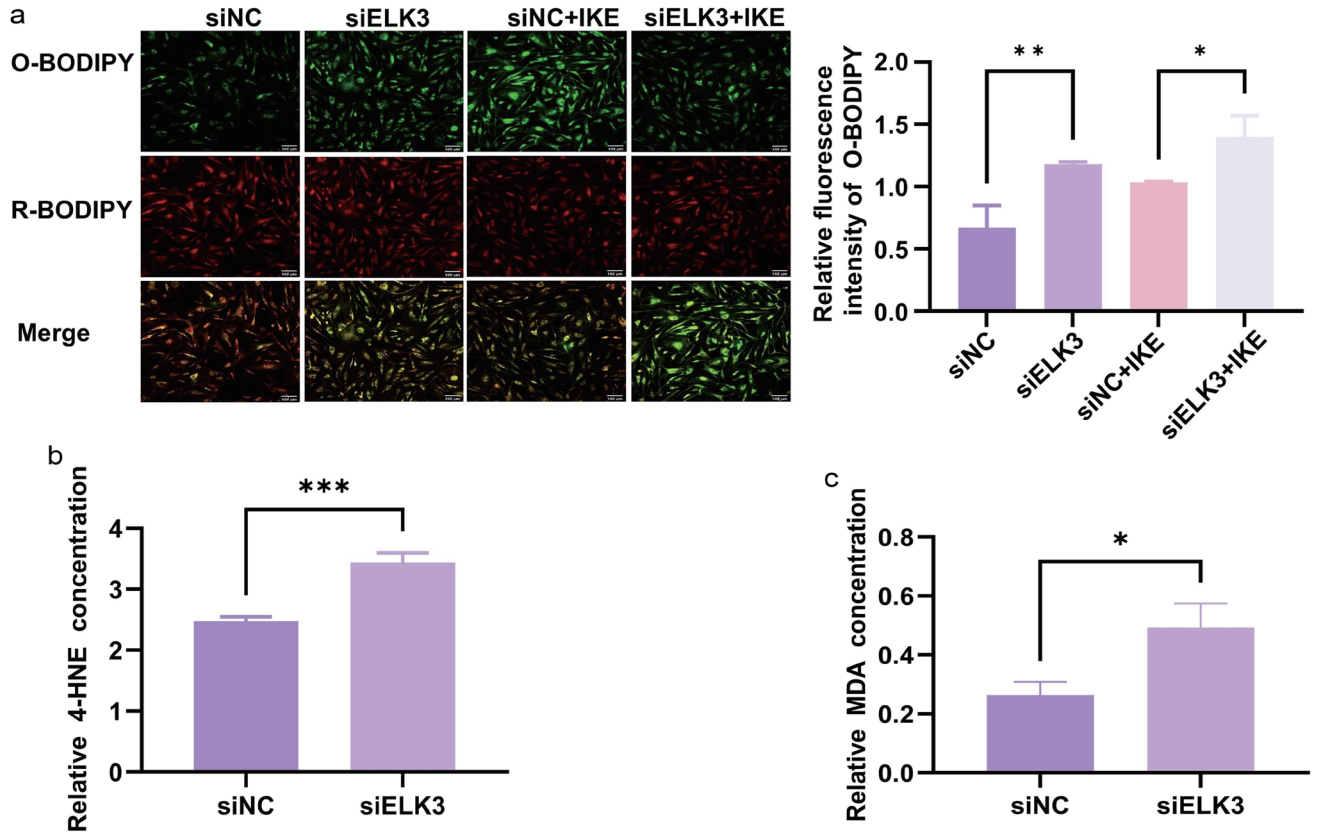

Fig. 3. Effect of ELK3 on lipid peroxidation in rheumatoid arthritis (RA) fibroblast-like synoviocytes (FLS). (a) Silencing ELK3 in RA FLS, with or without IKE induction, BODIPY C11 probe staining was performed. (b,c) The confocal microscope was used to observe the fluorescence intensity of oxidized (O-BODIPY) and reduced (R-BODIPY) states in RA FLS, and the ratio of oxidized to reduced states was calculated. Scale bar: 100 μm. ELISA kits were used to detect the levels of 4-HNE (b) and MDA (c) after silencing ELK3 in RA FLS. Results are expressed as mean ± SEM from three independent experiments: *$p < 0.05$, **$p < 0.01$, ***$p < 0.001$. 4-HNE, 4-hydroxy-2-nonenal; MDA, malondialdehyde;O-BODIPY, oxidized BODIPY; R-BODIPY, reduced BODIPY.

ever, these interventions primarily aim to alleviate symptoms and reduce side effects rather than cure the disease.[22] Consequently, identifying novel therapeutic targets and exploring the underlying molecular mechanisms are crucial for advancing RA treatment.

Ferroptosis is a distinct form of non-apoptotic cell death characterized by its dependence on iron, differing from traditional cell death pathways in terms of morphology, biochemistry, and genetics.[23,24] Recent studies have highlighted a significant relationship between ferroptosis and RA. For instance, iron deposits have been identified in both OA and RA, with RA exhibiting a higher accumulation of iron. Excessive iron accumulation in the synovium of RA patients promotes sustained inflammation, and under pro-inflammatory conditions, FLS exhibit hyperproliferation.[25] Moreover, ROS, as byproducts of oxidative stress, are abundant in the synovial cavities of RA patients. These ROS contribute to an altered local microenvironment in affected joints, leading to abnormal synovial cell proliferation and intensified inflammatory infiltration. Thus, inducing ferroptosis has emerged as a promising strategy for RA therapy.[10]

ELK3, a transcription factor, has garnered considerable attention in cancer research, where its dysregulated expression has been associated with alterations in key phenotypes, including cell migration, invasion, proliferation, cell cycle regulation, and apoptosis.[16] In this study, we compared ELK3 expression between RA and OA and found that ELK3 is significantly upregulated in RA. Based on this finding, we hypothesized that ELK3 may play a critical biological role in RA. RA FLS, which are pivotal in disease progression, exhibit rapid proliferation and an invasive phenotype. To investigate whether ELK3 influences RA FLS, we assessed its impact on their biological activity. Using Transwell assays, we demonstrated that silencing ELK3 significantly reduced the invasive capacity of RA FLS. Additionally, CCK-8 assays revealed that the proliferation of RA FLS was suppressed upon ELK3 knockdown. These results suggest that ELK3 contributes to RA pathogenesis by modulating the biological activity of RA FLS.

Although ELK3 is known to affect cellular biological activity, its role in ferroptosis has not been previously reported. In our study, we observed that ELK3 regulates RA FLS activity and influences key ferroptosis-related indicators, such as lipid peroxidation levels, Fe^{2+} content, and ROS production. These findings suggest a potential link between ELK3 and ferroptosis in RA FLS. Based on these observations, we propose that ELK3 may serve as a potential molecular target for RA therapy. However, the precise mechanisms by which ELK3 participates in ferroptosis require further investigation.

Nrf2 plays a critical role in inhibiting ferroptosis, and previous studies have suggested that RA is associated with increased oxidative stress, reduced antioxidant levels, and diminished antioxidant capacity.[26] However, recent studies have reported that Nrf2 expression is higher in RA synovial tissue and arthritis mouse

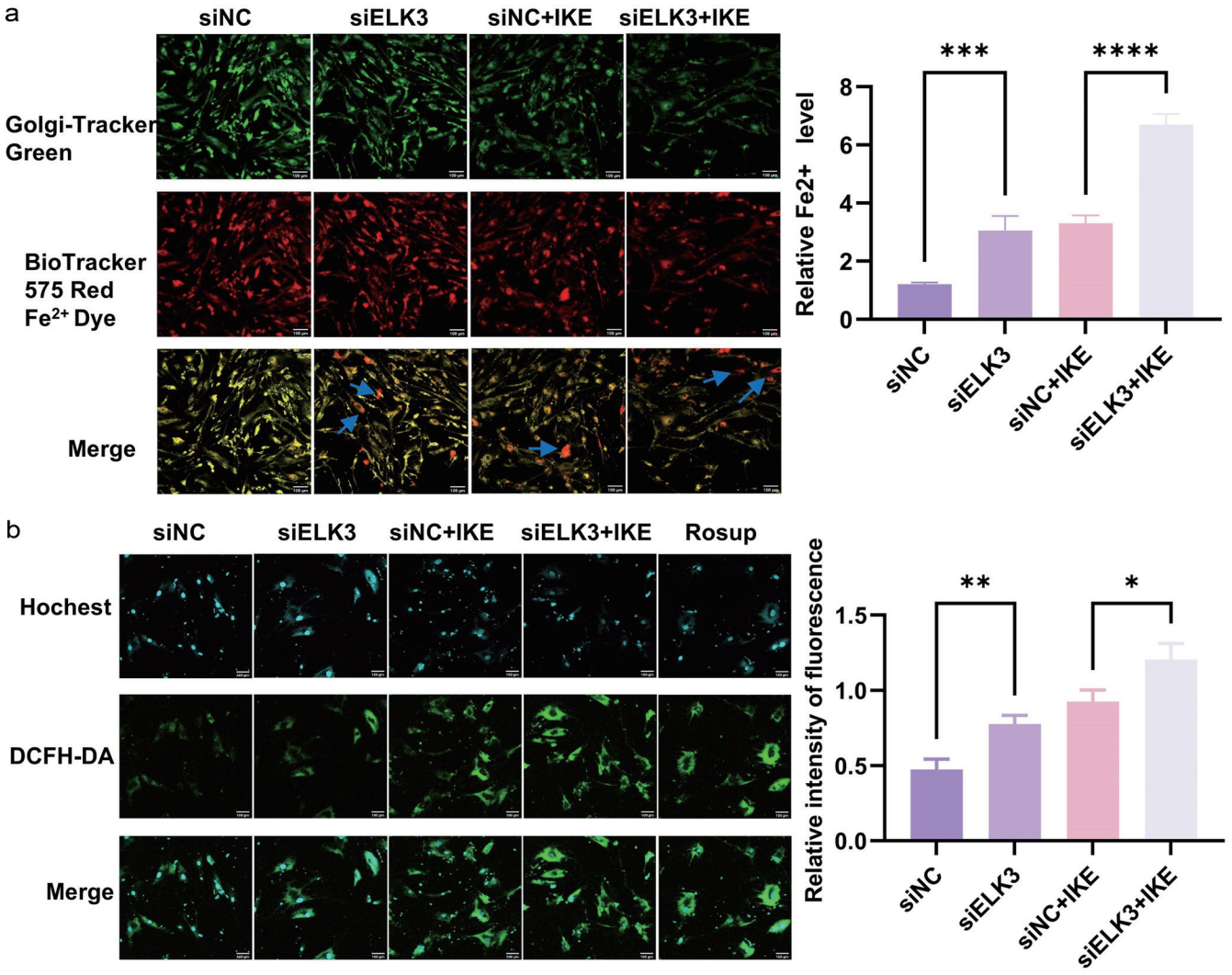

Fig. 4. Effect of ELK3 on Fe^{2+} and ROS levels in rheumatoid arthritis (RA) fibroblast-like synoviocytes (FLS). Fe^{2+} was detected using a ferrous ion probe, and ROS was detected using the DCFH-DA fluorescent probe in RA FLS, with or without IKE induction, after silencing ELK3 (a,b). Scale bar: 100 μm. Results are expressed as mean ± SEM from three independent experiments: *$p < 0.05$, **$p < 0.01$, ***$p < 0.001$. Golgi apparatus green: fluorescent probe; BioTracker 575 Red Fe^{2+} Dye: red ferrous dye; Hoechst: nuclear dye. DCFH-DA, reactive oxygen species (ROS) fluorescent probe.

models compared to normal controls, and RA FLS have lower lipid peroxidation levels than OA FLS.[27] The activity of Nrf2 is regulated by its protein stability, and Keap1 plays an important role in maintaining Nrf2 stability.[14]

Keap1, a member of the BTB-kelch protein family, is regulated through various mechanisms such as transcriptional control, epigenetic modifications, somatic mutations, post-translational modifications, and degradation.[28] Keap1 functions as a sensor for oxidative and electrophilic stress, and under oxidative stress conditions, the Keap1-Nrf2 pathway serves a protective role.[29] Keap1 is part of an E3 ubiquitin ligase complex that targets Nrf2 for ubiquitination and proteasomal degradation under normal conditions, strictly regulating Nrf2 activity.[30] Additionally, Nrf2 activation is regulated by p62, which is degraded via autophagy under normal conditions, but upregulated under oxidative stress, leading to Keap1 sequestration and activation of Nrf2-dependent antioxidant defense genes.[31] Studies have shown that the Keap1-Nrf2 pathway regulates the production of ROS in both the cytoplasm and mitochondria. When exposed to erastin, the p62 protein competitively binds with Keap1, releasing Nrf2, which enters the nucleus to activate downstream molecules such as NQO1, heme oxygenase-1, and ferritin heavy chain 1, participating in iron metabolism and lipid peroxidation.[32]

Our study found that the transcriptional repressor ELK3 can influence RA disease progression by inhibiting ferroptosis. We identified Keap1 as a potential downstream target of ELK3, and further experiments confirmed that ELK3 binds to the Keap1 promoter region. Based on previous reports,[15] ELK3 functions as a transcriptional repressor under basal conditions by binding to DNA. Therefore, we designed Keap1 mutants and performed dual-luciferase reporter gene experiments, finding that Keap1 activity was indeed reduced in the presence of ELK3. Western blot analysis showed that overexpression of ELK3 decreased Keap1 expression. Co-silencing Keap1 and ELK3 reversed the downregulation of downstream proteins NQO1, SLC7A11, and Nrf2 observed with ELK3 silencing alone. Thus, we conclude that ELK3 may regulate

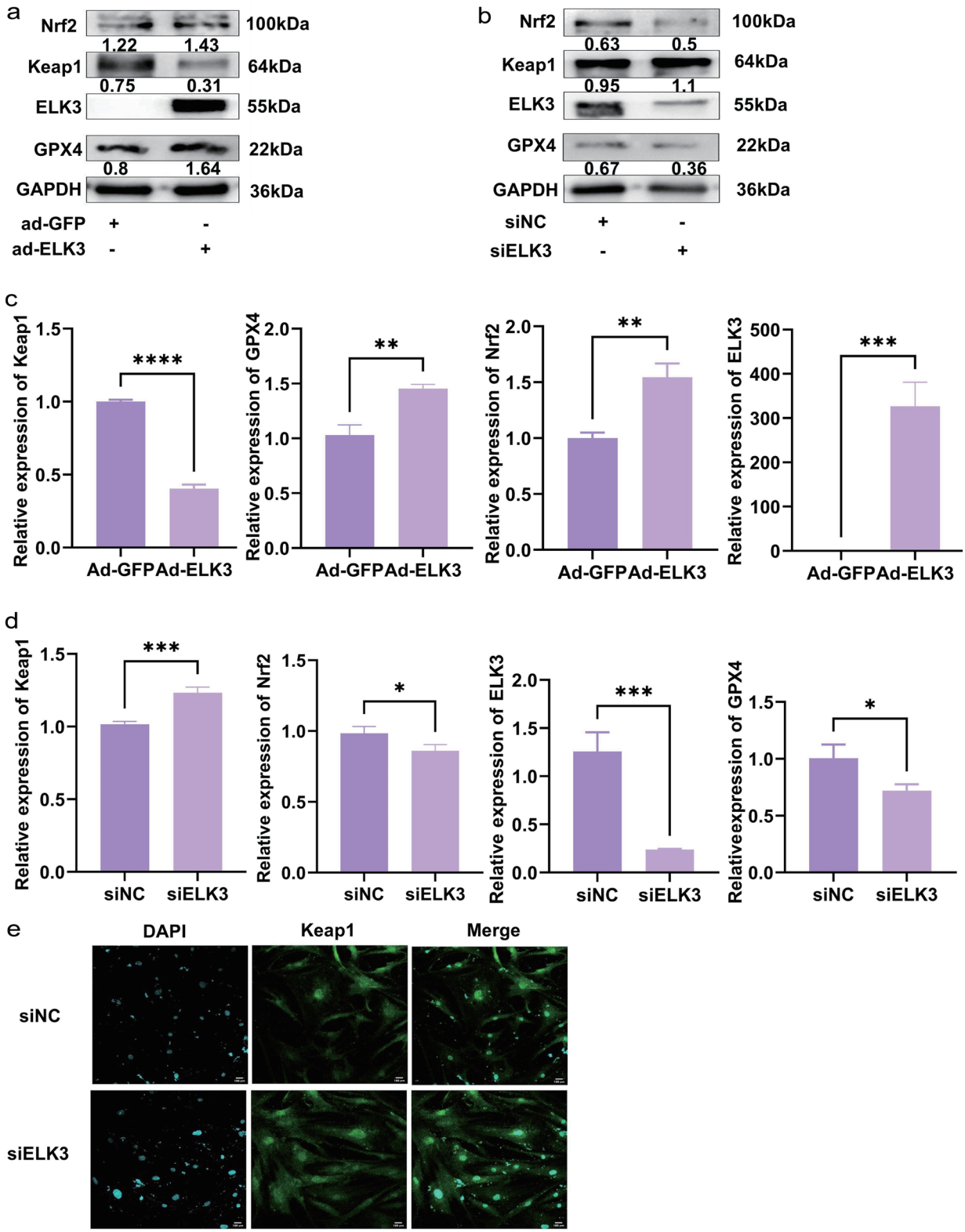

Fig. 5. ELK3 regulates ferroptosis-related markers. Western blot (a, b) and (c, d) real-time quantitative polymerase chain reaction (RT-qPCR) were used to detect the expression of ferroptosis-related molecules in rheumatoid arthritis (RA) fibroblast-like synoviocytes (FLS) after silencing or overexpressing ELK3. (e) Immunofluorescence was used to detect kelch-like ECH-associated protein 1 (Keap1) expression after silencing ELK3 in RA FLS. Results are expressed as mean ± SEM from three independent experiments: *$p < 0.05$, **$p < 0.01$, ***$p < 0.001$, ****$p < 0.0001$. SEM, standard error of the mean.

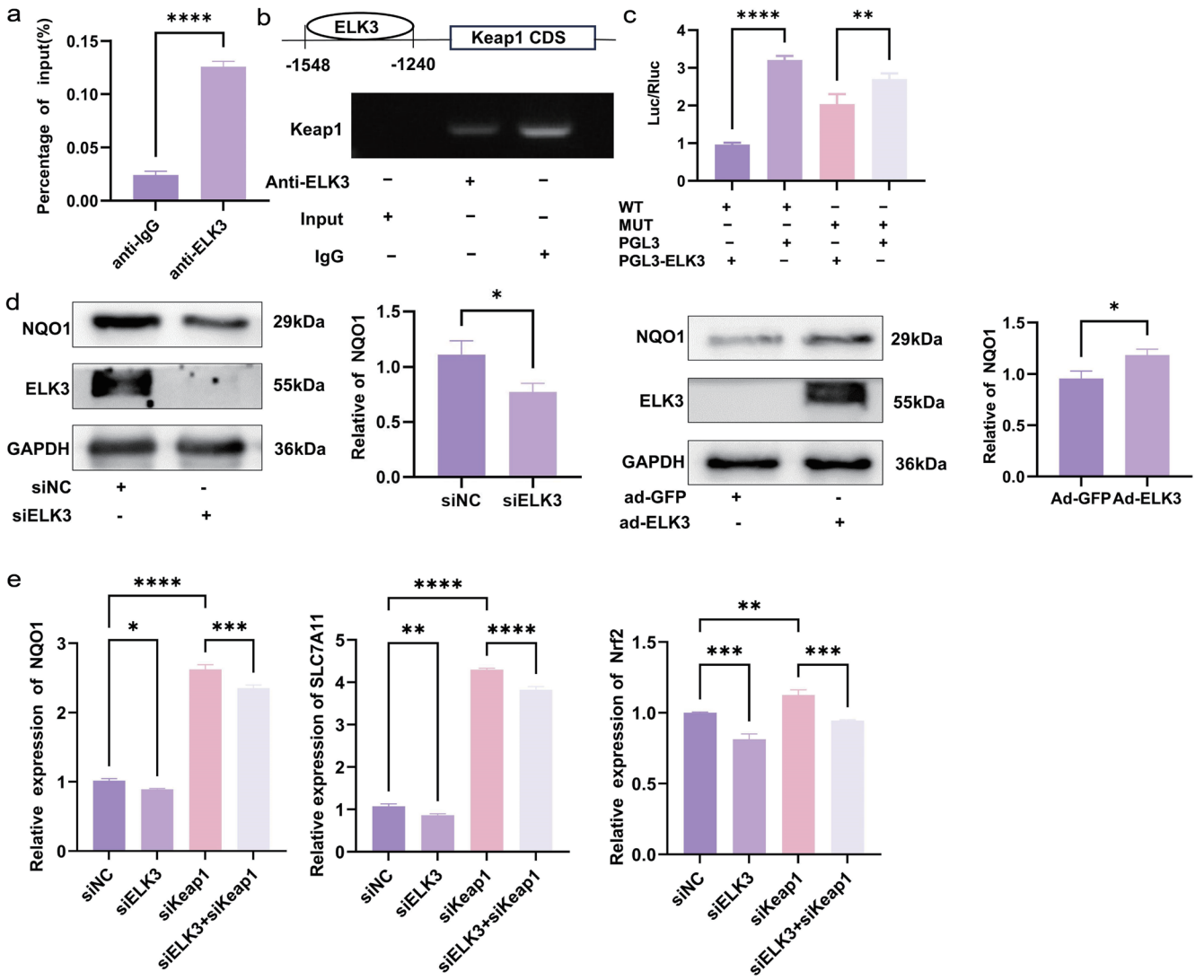

Fig. 6. ELK3 regulates ferroptosis in RA FLS by controlling kelch-like ECH-associated protein 1 (Keap1). (a, b) Chromatin immunoprecipitation polymerase chain reaction (ChIP-PCR) was used to detect the binding of ELK3 to the Keap1 promoter region. (c) A dual-luciferase reporter gene assay was used to detect the effect of ELK3 on the transcriptional activity of the Keap1 promoter. (d) Western blot was used to detect NAD(P)H quinone dehydrogenase 1 (NQO1) expression after silencing or overexpressing ELK3. (e) Real-time quantitative polymerase chain reaction (RT-qPCR) was used to detect the effect of silencing ELK3 alone or co-silencing ELK3 and Keap1 on the expression of NQO1, solute carrier family 7 member 11(SLC7A11), and nuclear factor erythroid 2-related factor 2(Nrf2). Results are expressed as mean ± SEM from three independent experiments: $*p < 0.05$, $**p < 0.01$, $***p < 0.001$, $****p < 0.0001$. SEM, standard error of the mean.

ferroptosis in RA FLS by modulating Keap1 expression.

In summary, this study identifies ELK3 as a potential pathogenic molecule in RA. It may influence disease progression by regulating the activity and ferroptosis phenotype of RA FLS, with Keap1 being a potential target molecule through which ELK3 exerts its effects. ELK3 binds to the promoter of Keap1, inhibiting its transcriptional activity, thereby affecting the expression of ferroptosis-related molecules and contributing to the progression of ferroptosis in RA FLS (Fig. 7). ELK3 has revealed a new pathogenic pathway for the progression of RA and may serve as a potential therapeutic target for RA treatment. Of course, our research has certain limitations. Although we have studied the role of ELK3 in ferroptosis in fibroblast-like synoviocytes in rheumatoid arthritis, *in vivo* animal experiments for further validation have not been conducted.

Future directions

Future research will focus on constructing gene knockout mice and establishing a collagen-induced arthritis mouse model. Micro-CT data analysis, tissue histopathology, and staining will be performed to further validate ELK3's role as a transcriptional repressor in RA progression, potentially identifying a novel pathogenic pathway.

Conclusions

This study identifies ELK3 as a potential pathogenic molecule in RA, suggesting that it may influence RA progression by regulating the activity of RA FLS. ELK3 can affect the ferroptosis phenotype, with Keap1 identified as a key target molecule through which ELK3 exerts its effects. These findings indicate that ELK3 could

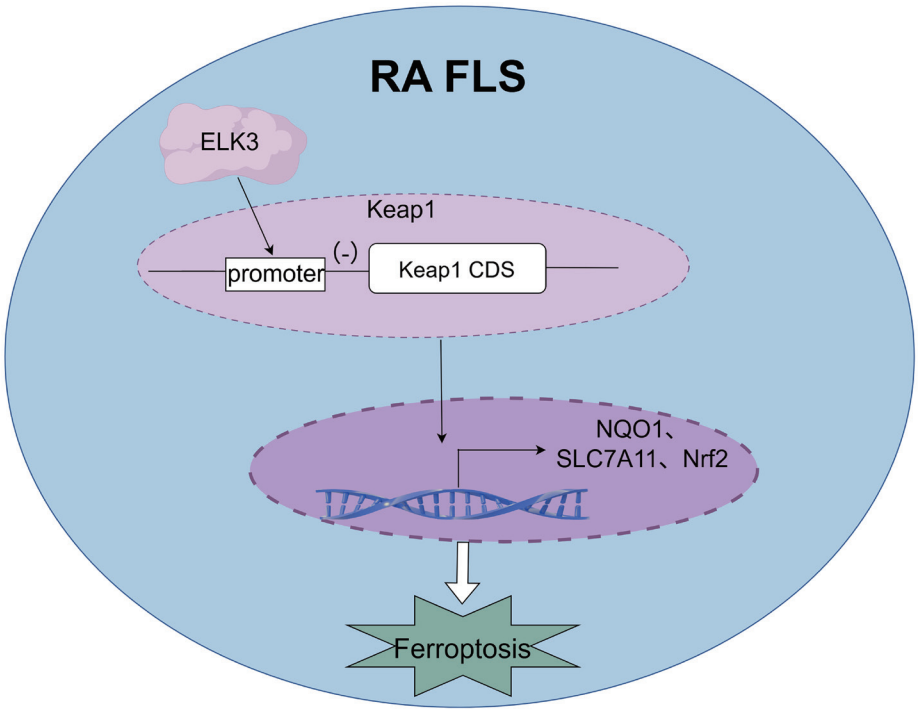

Fig. 7. ELK3 inhibits its transcriptional activity by binding to the kelch-like ECH-associated protein 1 (Keap1) promoter, affecting the expression of ferroptosis-related molecules. NAD(P)H quinone dehydrogenase 1 (NQO1), solute carrier family 7 member 11 (SLC7A11), and nuclear factor erythroid 2-related factor 2 (Nrf2), and involved in the progression of ferroptosis in rheumatoid arthritis (RA) fibroblast-like synoviocytes (FLS).

serve as a potential therapeutic target for RA.

Acknowledgments

We are very grateful for the help provided by the teachers and classmates in the laboratory. ChatGPT was used for grammatical and linguistic refinement during the drafting of this text.

Funding

This study was supported by the National Natural Science Foundation of China (Study on the Mechanism of E2F2 Regulating Rheumatoid Arthritis Synoviocyte Activity, 81671624) and the Shandong Natural Science Foundation (Role of EIF5A in Rheumatoid Arthritis Synovitis and Mechanism Study, ZR2023MH013).

Conflict of interest

The authors declare no conflicts of interest related to this publication.

Author contributions

All authors contributed to the writing or revision of the article. Research design (JHP), manuscript writing (YQZ), data acquisition and analysis (HMS, LW).

Ethical statement

The RA and OA synovial tissues used in this study were obtained from Shandong First Medical University's affiliated hospital. The study received informed consent from all patients and was approved by the Medical Ethics Committee of the Shandong Provincial Medical Biotechnology Research Center (Ethics Approval No.: 2014-2019). All patients met the 1987 revised RA diagnostic criteria established by the American College of Rheumatology. The research process complies with the principles of the Helsinki Declaration.

Data sharing statement

No additional data are available.

References

[1] Kumar LD, Karthik R, Gayathri N, Sivasudha T. Advancement in contemporary diagnostic and therapeutic approaches for rheumatoid arthritis. Biomed Pharmacother 2016;79:52–61. doi:10.1016/j.biopha.2016.02.001, PMID:27044812.
[2] Scherer HU, Häupl T, Burmester GR. The etiology of rheumatoid arthritis. J Autoimmun 2020;110:102400. doi:10.1016/j.jaut.2019.102400, PMID:31980337.
[3] Cush JJ. Rheumatoid Arthritis: Early Diagnosis and Treatment. Rheum Dis Clin North Am 2022;48(2):537–547. doi:10.1016/j.rdc.2022.02.010, PMID:35400377.
[4] Sun P, Su J, Wang X, Zhou M, Zhao Y, Gu H. Nucleic Acids for Potential Treatment of Rheumatoid Arthritis. ACS Appl Bio Mater 2022;5(5):1990–2008. doi:10.1021/acsabm.1c01205, PMID:35118863.
[5] Lefèvre S, Knedla A, Tennie C, Kampmann A, Wunrau C, Dinser R, *et al*. Synovial fibroblasts spread rheumatoid arthritis to unaffected joints. Nat Med 2009;15(12):1414–1420. doi:10.1038/nm.2050, PMID:19898488.
[6] Niu HQ, Zhao XC, Zhao WP, Li XF. [Metabolic changes of synovial fibroblasts and rheumatoid arthritis]. Zhonghua Nei Ke Za Zhi

2019;58(1):69–73. doi:10.3760/cma.j.issn.0578-1426.2019.01.013, PMID:30605955.
[7] Mueller AL, Payandeh Z, Mohammadkhani N, Mubarak SMH, Zakeri A, Alagheband Bahrami A, *et al*. Recent Advances in Understanding the Pathogenesis of Rheumatoid Arthritis: New Treatment Strategies. Cells 2021;10(11):3017. doi:10.3390/cells10113017, PMID: 34831240.
[8] Jang S, Kwon EJ, Lee JJ. Rheumatoid Arthritis: Pathogenic Roles of Diverse Immune Cells. Int J Mol Sci 2022;23(2):905. doi:10.3390/ijms23020905, PMID:35055087.
[9] Bottini N, Firestein GS. Duality of fibroblast-like synoviocytes in RA: passive responders and imprinted aggressors. Nat Rev Rheumatol 2013;9(1):24–33. doi:10.1038/nrrheum.2012.190, PMID:23147896.
[10] Zhao T, Yang Q, Xi Y, Xie Z, Shen J, Li Z, *et al*. Ferroptosis in Rheumatoid Arthritis: A Potential Therapeutic Strategy. Front Immunol 2022;13:779585. doi:10.3389/fimmu.2022.779585, PMID:35185879.
[11] Zhao H, Tang C, Wang M, Zhao H, Zhu Y. Ferroptosis as an emerging target in rheumatoid arthritis. Front Immunol 2023;14:1260839. doi:10.3389/fimmu.2023.1260839, PMID:37928554.
[12] Yazar M, Sarban S, Kocyigit A, Isikan UE. Synovial fluid and plasma selenium, copper, zinc, and iron concentrations in patients with rheumatoid arthritis and osteoarthritis. Biol Trace Elem Res 2005;106(2):123–132. doi:10.1385/BTER:106:2:123, PMID:16116244.
[13] Zhang C, Liu X, Jin S, Chen Y, Guo R. Ferroptosis in cancer therapy: a novel approach to reversing drug resistance. Mol Cancer 2022;21(1):47. doi:10.1186/s12943-022-01530-y, PMID:35151318.
[14] Yan R, Lin B, Jin W, Tang L, Hu S, Cai R. NRF2, a Superstar of Ferroptosis. Antioxidants (Basel) 2023;12(9):1739. doi:10.3390/antiox12091739, PMID:37760042.
[15] Giovane A, Pintzas A, Maira SM, Sobieszczuk P, Wasylyk B. Net, a new ets transcription factor that is activated by Ras. Genes Dev 1994;8(13):1502–1513. doi:10.1101/gad.8.13.1502, PMID:7958835.
[16] Yoo SM, Lee CJ, An HJ, Lee JY, Lee HS, Kang HC, *et al*. RSK2-Mediated ELK3 Activation Enhances Cell Transformation and Breast Cancer Cell Growth by Regulation of c-fos Promoter Activity. Int J Mol Sci 2019;20(8):1994. doi:10.3390/ijms20081994, PMID:31018569.
[17] Shergalis A, Bankhead A 3rd, Luesakul U, Muangsin N, Neamati N. Current Challenges and Opportunities in Treating Glioblastoma. Pharmacol Rev 2018;70(3):412–445. doi:10.1124/pr.117.014944, PMID:29669750.
[18] Park W, Chawla A, O'Reilly EM. Pancreatic Cancer: A Review. JAMA 2021;326(9):851–862. doi:10.1001/jama.2021.13027, PMID:34547082.
[19] Huang J, Fu X, Chen X, Li Z, Huang Y, Liang C. Promising Therapeutic Targets for Treatment of Rheumatoid Arthritis. Front Immunol 2021;12:686155. doi:10.3389/fimmu.2021.686155, PMID:34305919.
[20] Bullock J, Rizvi SAA, Saleh AM, Ahmed SS, Do DP, Ansari RA, *et al*. Rheumatoid Arthritis: A Brief Overview of the Treatment. Med Princ Pract 2018;27(6):501–507. doi:10.1159/000493390, PMID:30173215.
[21] Singh JA. Treatment Guidelines in Rheumatoid Arthritis. Rheum Dis Clin North Am 2022;48(3):679–689. doi:10.1016/j.rdc.2022.03.005, PMID:35953230.
[22] Radu AF, Bungau SG. Management of Rheumatoid Arthritis: An Overview. Cells 2021;10(11):2857. doi:10.3390/cells10112857, PMID: 34831081.
[23] Jiang X, Stockwell BR, Conrad M. Ferroptosis: mechanisms, biology and role in disease. Nat Rev Mol Cell Biol 2021;22(4):266–282. doi:10.1038/s41580-020-00324-8, PMID:33495651.
[24] Dixon SJ, Lemberg KM, Lamprecht MR, Skouta R, Zaitsev EM, Gleason CE, *et al*. Ferroptosis: an iron-dependent form of nonapoptotic cell death. Cell 2012;149(5):1060–1072. doi:10.1016/j.cell.2012.03.042, PMID:22632970.
[25] Nygaard G, Firestein GS. Restoring synovial homeostasis in rheumatoid arthritis by targeting fibroblast-like synoviocytes. Nat Rev Rheumatol 2020;16(6):316–333. doi:10.1038/s41584-020-0413-5, PMID:32393826.
[26] Mateen S, Moin S, Khan AQ, Zafar A, Fatima N. Increased Reactive Oxygen Species Formation and Oxidative Stress in Rheumatoid Arthritis. PLoS One 2016;11(4):e0152925. doi:10.1371/journal.pone.0152925, PMID:27043143.
[27] Wruck CJ, Fragoulis A, Gurzynski A, Brandenburg LO, Kan YW, Chan K, *et al*. Role of oxidative stress in rheumatoid arthritis: insights from the Nrf2-knockout mice. Ann Rheum Dis 2011;70(5):844–850. doi:10.1136/ard.2010.132720, PMID:21173018.
[28] Kopacz A, Kloska D, Forman HJ, Jozkowicz A, Grochot-Przeczek A. Beyond repression of Nrf2: An update on Keap1. Free Radic Biol Med 2020;157:63–74. doi:10.1016/j.freeradbiomed.2020.03.023, PMID:32234331.
[29] Yamamoto M, Kensler TW, Motohashi H. The KEAP1-NRF2 System: a Thiol-Based Sensor-Effector Apparatus for Maintaining Redox Homeostasis. Physiol Rev 2018;98(3):1169–1203. doi:10.1152/physrev.00023.2017, PMID:29717933.
[30] Baird L, Yamamoto M. The Molecular Mechanisms Regulating the KEAP1-NRF2 Pathway. Mol Cell Biol 2020;40(13):e00099–20. doi:10.1128/MCB.00099-20, PMID:32284348.
[31] Taguchi K, Fujikawa N, Komatsu M, Ishii T, Unno M, Akaike T, *et al*. Keap1 degradation by autophagy for the maintenance of redox homeostasis. Proc Natl Acad Sci U S A 2012;109(34):13561–13566. doi:10.1073/pnas.1121572109, PMID:22872865.
[32] Ou M, Jiang Y, Ji Y, Zhou Q, Du Z, Zhu H, *et al*. Role and mechanism of ferroptosis in neurological diseases. Mol Metab 2022;61:101502. doi:10.1016/j.molmet.2022.101502, PMID:35447365.